This manuscript has been authored by UT-Battelle LLC under Contract No. DE-AC05-00OR22725 with the U.S. Department of Energy. The United States Government retains and the publisher, by accepting the article for publication, acknowledges that the United States Government retains a non-exclusive, paid-up, irrevocable, world-wide license to publish or reproduce the published form of this manuscript, or allow others to do so, for United States Government purposes. The Department of Energy will provide public access to these results of federally sponsored research in accordance with the DOE Public Access Plan (http://energy.gov/downloads/doe-public-access-plan).

Lightweight TiC-(Fe-Al) ceramic-metal composites made in situ by pressureless melt infiltration

Corson L. Cramer[1,*], Makayla S. Edwards[2], Jacob W. McMurray[2], Amy M. Elliott[1], Richard A. Lowden[2]

[1]Energy & Transportation Science Division, Energy and Environmental Sciences Directorate, Oak Ridge National Laboratory, Oak Ridge, TN, USA

[2]Materials Science and Technology Division, Physical Sciences Directorate, Oak Ridge National Laboratory, Oak Ridge, TN, USA

*cramercl@ornl.gov

Abstract

Lightweight ceramic-metal (cermet) composites combine stiffness and hardness with fracture toughness and ductility. TiC and Al are ideal pairs among lightweight cermet composites because of their relatively high strength to weight ratios, but these materials are hard to process in solid state or with Al melt infiltration without making an aluminum carbide phase, which is detrimental to mechanical properties. In this research, Fe is added to a TiC powder preform to reduce the activity of Al with TiC during Al melt infiltration and to aid in pressing TiC preforms, making a lightweight TiC-(Fe-Al) composite while avoiding other, unwanted phases. The composites are made by first pressing TiC powder mixed with Fe followed by Al melt infiltration; the result is a composite with high TiC content in a two-phase matrix, both of which are Fe-Al-based. The composite has low density, low porosity, high hardness, no detectable Al_4C_3 phase with X-ray diffraction, and retains shape well during infiltration.

Keywords: Ceramic-metal (cermet) composites; Intermetallics; Melt infiltration; TiC

Introduction

Lightweight ceramic-metal (cermet) composites are of interest in many applications where a high strength-to-weight ratio is needed [1]. A cermet is comprised of a reinforcement ceramic phase higher than 50 vol.% and a metal phase, and typically the ceramic phase is continuous. TiC is an ideal ceramic reinforcement for a lightweight cermet. Al is ideal as a matrix material for lightweight cermets because it has low density, high strength-to-weight ratio, and high ductility. TiC and Al are an ideal pair for cermets in engineering design because of their individual strength-to-weight ratios [2], [3]. Combining the two materials would produce a lightweight cermet with ductility, stiffness, strength, and hardness beyond other cermet's [4], [5]. Unfortunately, infiltrating TiC with aluminum via melt infiltration to form a cermet usually results in the formation of an aluminum carbide phase at the interface of the two materials. Thus, developing a cermet based on this system that avoids aluminum carbide formation is advantageous for many applications.

TiC-Al composites can be made by capillary infiltration of TiC powder preforms with Al because Al wets TiC when high enough temperatures and times are used [6], [7]. Capillary infiltration makes cermets when a porous preform is in contact with a molten metal because the metal is drawn into the preform via wetting and surface tension forces, which drive capillary infiltration. TiC-Al

composites have been made this way [8]–[12], but with the formation of the Al_4C_3 phase at the TiC and Al interface, and this composite is not useful in most applications since Al_4C_3 degrades when exposed to atmospheric temperature and pressure [12]–[14]. To explain the chemistry, Al is known to form Al_4C_3 by depleting the TiC of its carbon to a molar ratio of around 0.95, and the remaining TiC_x is known to be stable even with sub-stoichiometry as denoted in Eq. 1 [15], [16]. Another impactful method to make TiC-Al composites is with combustion synthesis of carbon, Ti, and Al, but there is some residual Al_3Ti [17].

$$xTiC + Al \rightarrow \left(\frac{1-x}{4}\right) Al_4C_3 + xAl + TiC_x \text{, where } 0.9 < x < 0.95 \quad (1)$$

Additives in alloy and intermetallic form have been used to mitigate the Al_4C_3 formation by lowering the activity of molten Al with TiC. There have been large efforts to make intermetallic matrix composites to mitigate unwanted phases formed and increase the hardness and mechanical properties of cermets [18]–[21], but it is more difficult to stabilize the phases of intermetallics during processing [22], [23], especially when melting occurs. Studies showed that little to no Al_4C_3 formed when infiltrating TiC with $NiAl_3$ intermetallic, which is due to the higher reaction potential of Al and Ni over Al and carbon [24]–[26]. Also, adding Mg or Cu to Al has been known to aid in infiltration by lowering the Al melting temperature and increasing wettability of Al into TiC. This helps to decrease the infiltration temperature and time and, therefore, the Al/carbon reaction potential [11], [27], but more strategic additives can improve processing to provide a lightweight, strong matrix. Adding a material like Fe to the system can help process TiC-Al cermets because Fe makes the Al less active with the TiC and can provide a matrix with Al that is hard, lightweight, and strong. When Fe is present during processing, it can form with Al in the matrix phase to form a lightweight intermetallic suitable for composites. Also, it was shown that Fe and Al are compatible for processing together with Ti and carbon to form favorable products of TiC and Fe-Al matrix phases *in situ* [28], [29]. For these reasons, it is thought that adding Fe to the processing can mitigate Al_4C_3 formation and produce favorable phases. Additionally, melt infiltration of the intermetallic FeAl into TiC has been done but requires the green part shaping with wax or polymer as well as very precise elemental control of the FeAl [30], [31]. However, a potentially faster, cheaper, and more controlled method to make TiC composite with FeAl matrix and high TiC content is to add Fe to the TiC preforms and subsequently melt Al into the structure to obtain an Fe-Al matrix because raw materials are used and no extra steps are added to the pressing and infiltration process.

In this research, Fe is added to TiC powder. This is different compared to other studies because the Fe serves several purposes. The TiC/Fe powders are pressed together without wax or polymer binder because the Fe helps bind the TiC. The pressing of mixed preforms has been done with WC/Fe that were subsequently infiltrated with Ni [32]. Further, Fe helps draw the molten Al into the preform because Al wets Fe better than it wets TiC [33], [34]. It is also likely that there is improved wetting of Al onto TiC because of Fe coating the TiC from pressing or being in contact with TiC providing a local superheated exotherm of (Al+Fe). The Fe also mitigates the Al_4C_3 formation and combines with Al *in situ* to make a matrix consisting of the two elements. This yields a TiC-(Fe-Al) composite system that can be used mechanically without degrading due to

Al_4C_3 reaction when exposed to atmosphere and represents a cermet with low density and high hardness.

Materials and Methods

Stoichiometric TiC powder (-100+325 mesh, D_{50}~120 micron) and Fe powder (-325 mesh, D_{50}~20 micron) from Atlantic Equipment Engineers were used for preforms. Pure Al shot (Alfa Aesar, 99.99% purity) was used for infiltration. TiC and Fe powders in a ratio of 5:1, respectively, were roller milled with WC media in a plastic container placed on rollers for 1 hour to evenly mix the Fe into the TiC and encourage Fe coating onto TiC powders. This ratio was chosen because it allows Fe particles to pack around larger TiC particles and the Fe is a small enough amount compared to the Al infiltration that the phases formed should be on the Al-rich side of the Fe-Al phase diagram.

1 g of the mixed TiC/Fe powder was pressed with a steel die to 100 MPa. The iron serves as the binder for the TiC by allowing the TiC/Fe sample to be pressed, consolidated, and easily extracted from the die and transferred to a crucible without added polymer or wax binder, eliminating the need for a debinding step. The good consolidation of preforms is most likely due to Fe deforming and interlocking TiC particles. 0.18 g of Al is loaded on top of the TiC/Fe preform in an amount corresponding to the void space porosity of the TiC/Fe preform. A schematic of the setup is shown in Figure 1. The heating schedule was 1400°C at 10°C/min with 30 min. hold while flowing 300 ccm of Ar/4%H_2 in an alumina tube furnace.

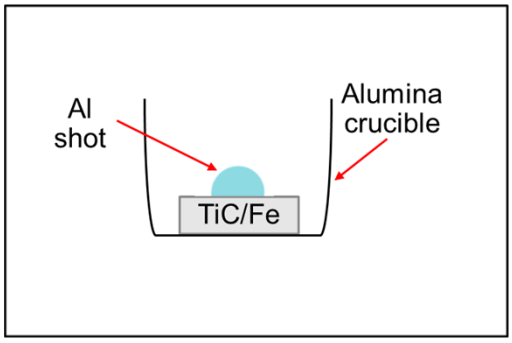

Figure 1: Schematic of processing setup.

The specimen microstructures were analyzed with SEM using a Hitachi S4800 microscope in secondary electron imaging mode. Geometric and Archimedes densities were measured when appropriate by measuring the part dimensions, dry mass, and submerged mass. Areal density was measured using ImageJ software on SEM cross-sections. Optical images were taken using a Leica DM4000 M LED system where computational stitching of the images is used to display full cross-sections.

Phase composition was determined by X-ray diffraction (XRD) using a PANalytical X'pert diffractometer with Mo K-α radiation (λ=0.709319 Å). The operating parameters were 40 kV and 40 mA with a 2θ step size of 0.02. The XRD patterns were analyzed using the whole pattern fitting approach with MDI Jade 2010 software database. Vickers hardness measurements were performed using a LECO LM 110AT apparatus under a 1.0 kgf load. The chemistry was predicted using

FactSage software and database. Simultaneous thermal analysis (STA) data, which consists of differential thermal analysis (DTA) and thermogravimetric analysis (TGA), were performed on TiC and Fe powders and Al shot packed in a crucible using a Netzsch STA 449 F3 Jupiter. The STA analysis of the TiC powder, Fe powder, and Al shot mixture was gathered to understand the thermodynamic stages of the materials during heating such as melting, reacting, and phases formed. The sample setup in STA analysis was not entirely analogous to the infiltration process because the TiC and Fe were not pressed together in a pellet as they are when they are pressed and infiltrated. However, the results should still reveal the thermodynamic reactions that occur during processing.

Results

Figure 2 shows an XRD pattern of the composite cross-section, which exhibited successful infiltration because Al fully penetrated the TiC/Fe preform. TiC, FeAl, α-Fe, and γ-Fe phases were detected. α-Fe is the phase that can dissolve higher amounts of Al than γ-Fe, but that dissolution behavior is opposite for carbon solutions such as steel. According to the XRD data, there was an absence of Al_4C_3. Also, the XRD confirmed that Fe formed with the Al to make some intermetallic *in situ*. It is also important to note that high density and consolidation occurred when processing in Ar/4%H_2 gas and did not occur when processing in Ar nor vacuum of 10^{-4} Torr.

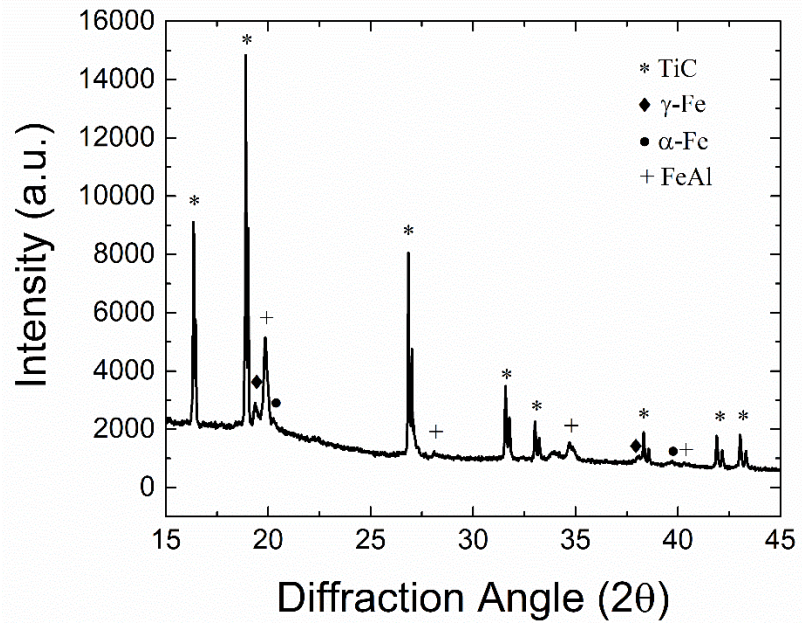

Figure 2: XRD pattern of the TiC-Fe-Al composite.

Figure 3 shows the STA data. Three peaks are shown in the DTA plot, two at 649°C and one at 1126.5°C. At 649°C, the DTA plot shows one endothermic peak followed immediately by an exothermic peak. The endothermic peak at 649°C is most likely the melting of Al and the exothermic peak after this is most likely the formation of Fe-Al intermetallic since this is a favorable reaction at this temperature when adding Fe into molten Al. The DTA plot also shows one endothermic peak at 1126.5°C, which is most likely the melting of this intermetallic. The mass

gain in the TGA data must be from reaction with the atmosphere because Al is known to oxidize even at significantly low partial pressures of O_2.

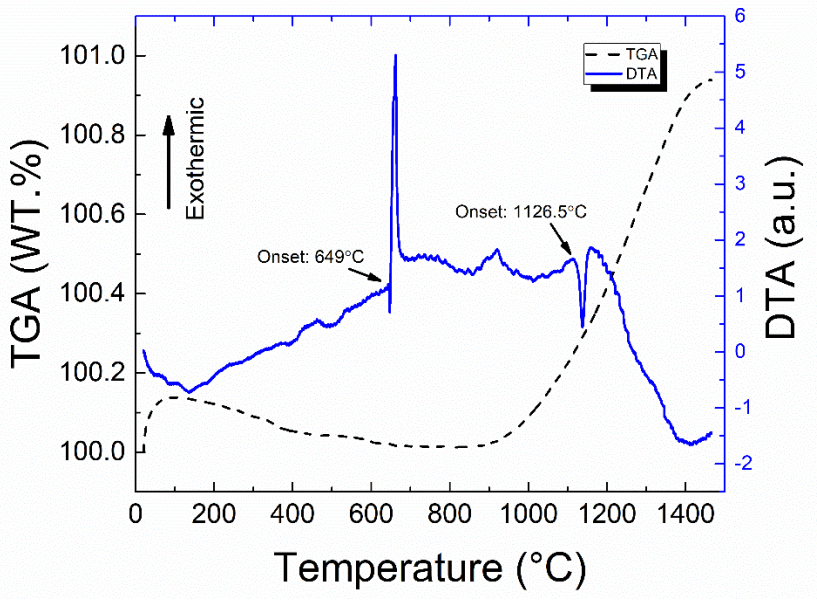

Figure 3: STA data of the TiC and Fe powders with Al shot showing the TGA and DTA during the heating cycle.

Figure 4 shows a macro image and optical image of the processed composite pellet. The pellet retains its puck-shaped geometry during processing as shown in Figure 4A. In Figure 4B, there is some porosity, the dark spots, in the part due to Ar/4%H_2 getting trapped during infiltration and dissolved H_2 gas coming out of solution during cooling. It should be noted that pure Ar and vacuum are not adequate atmosphere for consolidating these materials, so the H_2 gas helps the processing. The microstructure consists of a high content of TiC reinforcement as shown as the darker gray area in Figure 4B.

Table 1 shows the density, porosity, hardness, and dimensional change. The density is measured with areal and geometric techniques, but a theoretical density is not identified because amounts of each phase are challenging to quantify since it is not as simple as calculating the density based on a rule of mixtures for the amounts of TiC, Fe, and Al used in the current research. The porosity is measured with areal techniques and the density is measured with Archimedes techniques to indicate a quantity of residual pores from infiltration. The density is decreased compared to other composites with similar reinforcement content, which is most likely due to lightweight matrix material instead of heavier matrices of Fe and Ni. Also, the change in diameter and height are noted from green to infiltrated. The change in dimension is very low with only 1–3% change, which means there is limited shrinkage from solidification and volumetric changes during reaction of new phases.

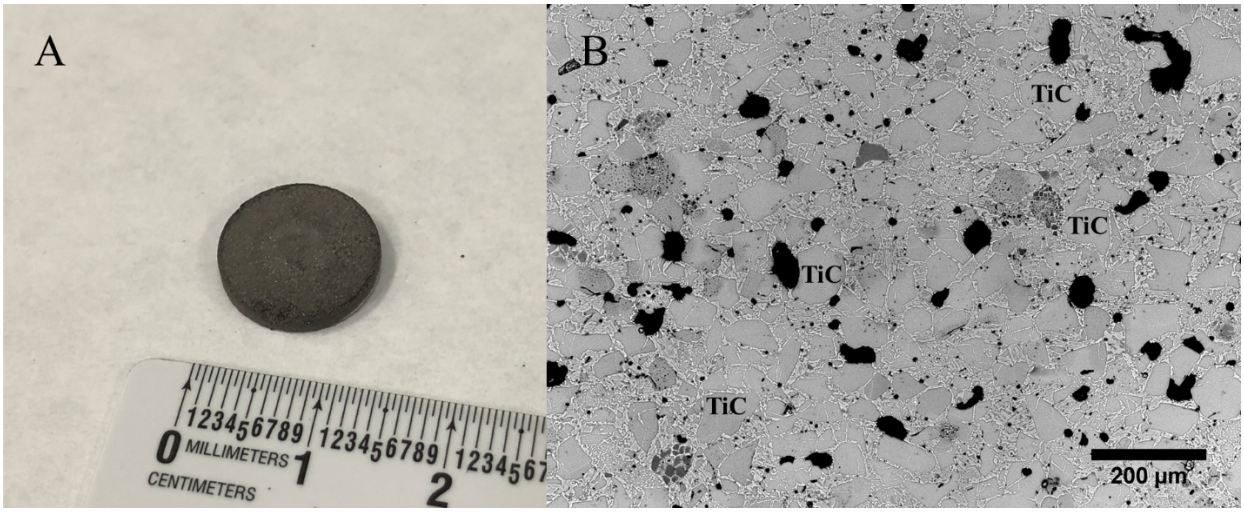

Figure 4: A) Macro image of composite pellet and B) optical image of the pellet cross-section.

Table 1: Properties of processed composite.

Property	Result
Density (g/cm3)	4.7
Porosity (%)	4.3
Hardness (GPa)	12.2±0.4
Change in diameter (%)	3.0%
Change in height (%)	1.0%

Figure 5 shows SEM images and EDS scans of the microstructure in secondary electron mode. Figure 5A shows the microstructure in one magnification, and Figure 5B shows an area in Figure 5A with higher magnification to further analyze the matrix material. The dark gray particles are TiC, but the matrix is comprised of multiple phases. The light gray material in the matrix is an Al-rich phase and the white lathes in the matrix are Fe-rich phases. It is likely that the Fe-rich phase is solid solution of Al in Fe and that the phase with more Al is FeAl. The lamellar microstructure resembles a FeAl + $FeAl_2$ eutectoid found in the Fe-Al system [35]–[37], but none of the other data gathered in this research provides evidence of the $FeAl_2$ phase.

With the EDS data and the XRD pattern, it is concluded that the darker Al-rich matrix phase, spot 1 in Figure 5, is FeAl. This is because this phase has higher Al content compared to the lathes and the XRD detects a significant amount of FeAl intermetallic. The white, Fe-rich lathes, spot 2 in Figure 5, are possibly both α-Fe or γ-Fe.

Once the melt starts to solidify, the FeAl is stable and the rest of the matrix forms because there is still excess Al and some Fe present. There could also be a small amount of carbon present from TiC becoming sub-stoichiometric at 1400°C [38]. The Al dissolves in Fe in the α-Fe phase and the carbon dissolves in the γ-phase during the solidification, and these two structures precipitate out into lathes much like a eutectoid microstructure. Smaller TiC particles seem to agglomerate together into clusters of TiC and matrix. This is either from TiC fines redistributing during infiltration in the molten infiltrant or from dissolution and reprecipitation of TiC particles.

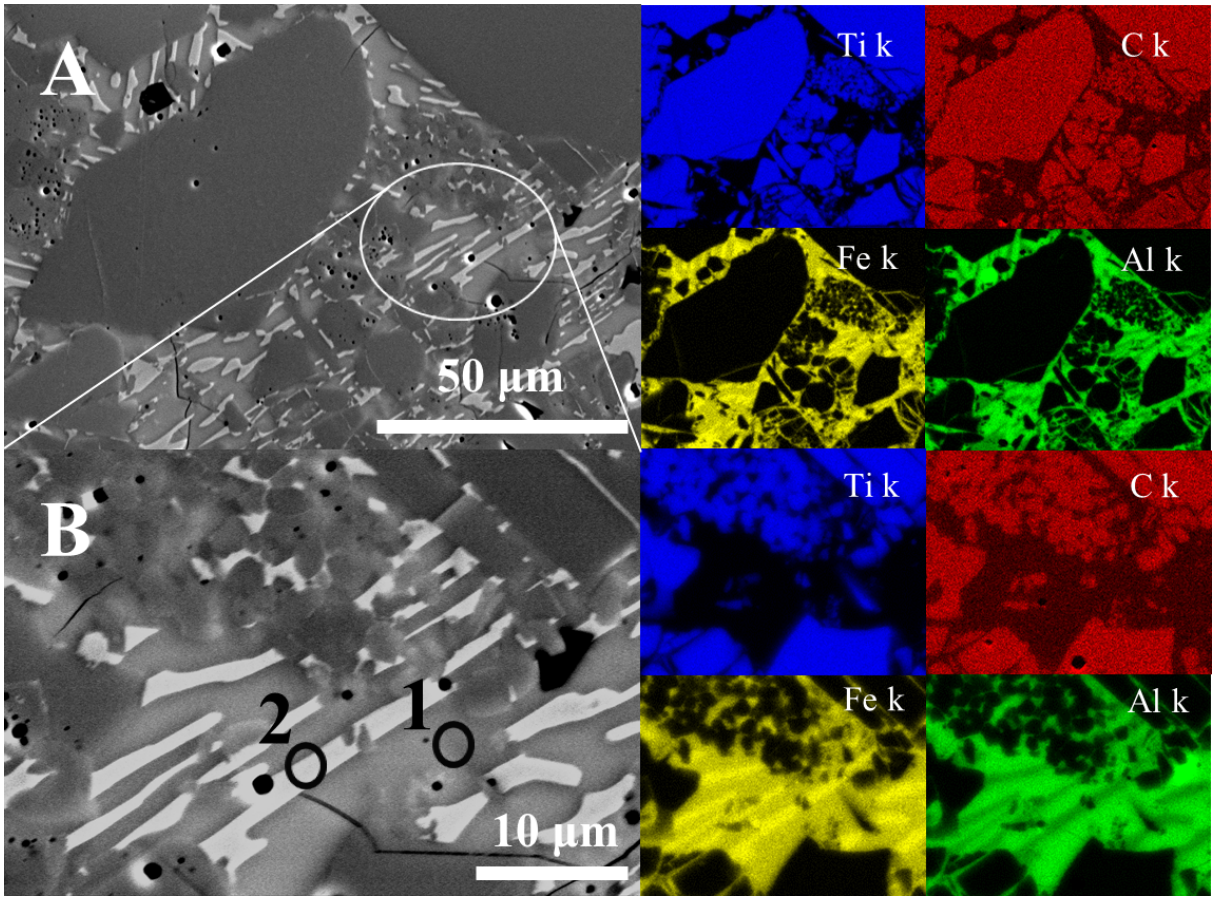

Figure 5: SEM images and EDS scans of the composite cross-section in secondary electron mode where B is a higher magnification image and EDS of an area in A. Spot 1 is FeAl, and spot 2 is Fe with some dissolved Al.

The hardness is 12.2 GPa as noted in Table 2. During hardness testing, some of the indents land on or close to the TiC particles as shown in Figure 6. Some indents from microhardness are shown in Figure 6, and they show how the cracks are arrested in TiC particles and how cracks deflect and arrest in the matrix, either at lamella of Fe-Al phases or up to TiC particles.

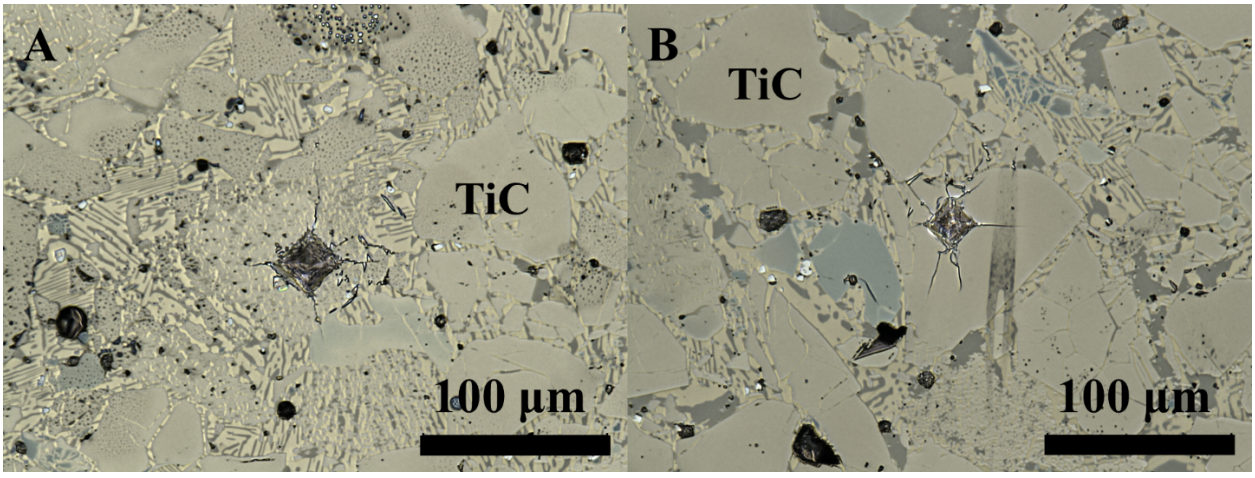

Figure 6: Optical images of microhardness indents on A) a cluster of smaller TiC particles and B) a larger TiC particle.

Discussion

Pressing and Shaping

The addition of Fe to TiC preforms allows the TiC/Fe mixture to press and consolidate enough in the green state to transfer from die to crucible without compromising the shape. Typically, a green part of TiC is too brittle to handle unless mixed with wax or polymer binder, but it must be transferred to a crucible for binder burn out, thereby adding another processing step. When pressing TiC with Fe, the Fe acts as a binder allowing the preform to be transferred from die to crucible without breaking the part. This was expected because the Fe is relatively soft compared to TiC. Pressing Fe and TiC together acts similar to a cold weld resulting in excellent pressing of the TiC/Fe green part [39]. Additionally, once the part is placed in the furnace and the Al melts into the preform, the composite pellet is near net shape with shrinkage of only 1–3%. Limited shrinkage occurs because the preform void space is completely filled with melt and, thus, there is no need to liquid phase sinter. The only shrinkage is from solidification of the melt and volume changes from phase formation, which are low. This means that this method should work with all types of additive manufacturing techniques in which a TiC/Fe preform is achievable.

Protection of TiC Particles and Matrix Formation

TiC and FeAl phases identified in the XRD were expected based on the known reactivities, but the α and γ Fe phases were not expected because the phase diagram shows that the amounts of Fe and Al used in this study should form $FeAl_2$ and Fe_2Al_5. Based on the XRD data, the formation of Al_4C_3 is limited because it is not detected in the XRD pattern. Further, based on the SEM images, there are no phases of Al_4C_3 visible. Also, the only phases around the TiC are Fe- and Al-based phases. It can be deduced from the XRD and SEM data that the TiC particles are protected from Al forming Al_4C_3 by means of Fe incorporation. To further understand the formation, reaction thermodynamics were simulated. For the given molar amounts of material processed in this research at 1400°C, the reaction was simulated using FactSage software in Eq. 2. From Eq. 2 and the molar amounts used in the current study, the available thermodynamic data predicted a small amount of Al_4C_3 formation, sub-stoichiometric TiC, and liquid melt of Fe-Al [40]–[42]. When comparing the molar amounts used in the current research but without Fe in Eq. 2, the Al_4C_3 formation is about 0.27 mol, whereas with Fe addition, the molar amount of Al_4C_3 is 0.017 mol. Based on this predicted chemistry, less Al_4C_3 formation occurred compared to TiC-Al composites. Also, during the infiltration process, the molten Al formed with Fe *in situ* to make a mostly two-phase matrix; the XRD data shows one intermetallic and two Fe phases form in the composite and the SEM image shows the two different matrix phases. One intermetallic is preferred, but when processing in TiC, the matrix formation is more complicated.

The phase formation in the matrix most likely proceeds in the following fashion. From the STA taken in the current research, Al melts at 649°C. The molten Al will start to infiltrate the TiC/Fe preform at this time. Almost directly after melting the Al, the STA data shows formation of a new material, which is most likely the formation of $FeAl_2$ and Fe_2Al_5. After this occurs, the sample is

most likely a porous, solid composite of TiC, $FeAl_2$, and Fe_2Al_5. Then, at 1126.5°C, STA shows another melting event, which is most likely these two intermetallics melting. Once the intermetallics are completely melted at 1400°C, the molten material finishes infiltration, surrounding the TiC particles even further. At 1400°C, the system is fully infiltrated and exists as TiC_x, carbon, and Fe-Al melt [38]. The whole system is cooled slowly to room temperature, where the lamellar eutectoid structure starts to form. During the cool down, the FeAl is stable but has too much Fe, so the formation of Fe lathes as Fe(C) and Fe(Al) occurs. The FeAl solidifies with Fe lathes intertwined. The exact mechanism of the formation is unknown, but the extra Al and small amount of carbon is most likely dissolved in the Fe lathes. The Al-rich, $FeAl_2$ and Fe_2Al_5, phases are also known to have high hardness, which makes them highly compatible with TiC composites for wear and hardness applications [43], [44]. The hardness values of the current research are comparable to FeAl intermetallic composites with TiC processed with melt infiltration methods [30], [31]. While more compositions of varying Fe would help identify how the microstructure develops or even stabilize the FeAl phase, they were not tested because the process is still being developed. Also, a better way to cover and protect the TiC must be sought with Fe coatings. Another improvement is the porosity, which might be improved if vacuum is used instead of flowing gas. It would also be interesting to monitor the infiltration in situ with XRD or other characterization to fully verify the processing steps.

$$TiC + 0.48Al + 0.21Fe \rightarrow 0.017Al_4C_3 + TiC_{0.95} + (Fe_{0.21}Al_{0.41})_{liq} \quad (2)$$

Conclusions

A lightweight composite with high reinforcement content was fabricated with TiC, Fe, and Al. The preforms of TiC and Fe were lightly pressed and subsequently melt infiltrated with molten Al to form a mostly two-phase matrix. The matrix phases were identified as FeAl and Fe. The processing thermodynamics with DTA were examined to help understand the matrix formation. Microstructural characterization and hardness of the composite are presented. Properties including density, hardness, and dimensional change were measured, which are 4.7 g/cm3, 12.2 GPa, and 1–3%, respectively. This material is promising for composites with high hardness, low density, and net shaping. This material could be used in lightweight aerospace applications as well as armor.

Acknowledgements

The authors would like to thank Olivia Shafer for assistance in editing. Research sponsored by the U.S. Department of Energy, Office of Energy Efficiency and Renewable Energy, Advanced Manufacturing Office, under contract DE-AC05-00OR22725 with UT-Battelle, LLC.

References

[1] S. P. Rawal, “Metal-matrix composites for space applications,” *JOM*, vol. 53, no. 4, pp. 14–17, Apr. 2001.

[2] I. A. Ibrahim, F. A. Mohamed, and E. J. Lavernia, “Particulate reinforced metal matrix composites ? a review,” *J. Mater. Sci.*, vol. 26, no. 5, pp. 1137–1156, 1991.

[3] F. Delannay, L. Froyen, and A. Deruyttere, “The wetting of solids by molten metals and its relation to the preparation of metal-matrix composites composites,” *J. Mater. Sci.*, vol. 22, no. 1, pp. 1–16, Jan. 1987.

[4] D. Richerson, *Modern ceramic engineering: properties, processing, and use in design*. 2005.

[5] D. Vallauri, I. C. Atías Adrián, and A. Chrysanthou, “TiC-TiB 2 composites: A review of phase relationships, processing and properties,” *J. Eur. Ceram. Soc.*, vol. 28, pp. 1697–1713, 2008.

[6] S. K. RHEE, “Wetting of Ceramics by Liquid Aluminum,” *J. Am. Ceram. Soc.*, vol. 53, no. 7, pp. 386–389, Jul. 1970.

[7] Q. Lin, P. Shen, L. Yang, S. Jin, and Q. Jiang, “Wetting of TiC by molten Al at 1123–1323K,” *Acta Mater.*, vol. 59, no. 5, pp. 1898–1911, Mar. 2011.

[8] E. . Aguilar, C. . León, A. Contreras, V. . López, R. A. . Drew, and E. Bedolla, “Wettability and phase formation in TiC/Al-alloys assemblies,” *Compos. Part A Appl. Sci. Manuf.*, vol. 33, no. 10, pp. 1425–1428, Oct. 2002.

[9] D. Muscat, K. Shanker, and R. A. L. Drew, “Al/TiC composites produced by melt infiltration,” *Mater. Sci. Technol.*, vol. 8, no. 11, pp. 971–976, Nov. 1992.

[10] J. C. Viala, M. Peronnet, F. Bosselet, and J. Bouix, “CHEMICAL COMPATIBILITY BETWEEN ALUMINIUM BASE MATRICES AND LIGHT REFRACTORY CARBIDE REINFORCEMENTS.”

[11] K. B. Lee, H. S. Sim, and H. Kwon, “Reaction products of Al/TiC composites fabricated by the pressureless infiltration technique,” *Metall. Mater. Trans. A*, vol. 36, no. 9, pp. 2517–2527, Sep. 2005.

[12] A. R. Kennedy, D. P. Weston, and M. I. Jones, “Reaction in Al–TiC metal matrix composites,” *Mater. Sci. Eng. A*, vol. 316, no. 1–2, pp. 32–38, Nov. 2001.

[13] V. H. López and A. R. Kennedy, “Flux-assisted wetting and spreading of Al on TiC,” *J. Colloid Interface Sci.*, vol. 298, no. 1, pp. 356–362, Jun. 2006.

[14] E. Trujillo-Vázquez, M. I. Pech-Canul, S. A. Gallardo-Heredia, and J. C. Flores-García, “Behavior of Al_4C_3 in Al/TiC Composites Under Controlled Humid Environment,” in *TMS2013 Supplemental Proceedings*, Hoboken, NJ, USA: John Wiley & Sons, Inc., 2013, pp. 1085–1093.

[15] J. Viala, M. Peronnet, and F. Bosselet, “Chemical compatibility between aluminum base matrices and light refractory carbide reinforcements,” *JC Viala, P. Fortier, J.*, 1998.

[16] V. I. Kononnako, G. P. Shveikin, A. L. Sukhman, V. I. Lomovtsev, and B. V. Mitrofanov, “Chemical compatibility of titanium carbide with aluminum, gallium, and indium melts,” *Sov. Powder Metall. Met. Ceram.*, vol. 15, no. 9, pp. 699–702, Sep. 1976.

[17] G. Xiao, Q. Fan, M. Gu, and Z. Jin, “Microstructural evolution during the combustion synthesis of TiC–Al cermet with larger metallic particles,” *Mater. Sci. Eng. A*, vol. 425,

no. 1–2, pp. 318–325, Jun. 2006.

[18] C. M. Ward-Close, R. Minor, and P. J. Doorbar, “Intermetallic-matrix composites—a review,” *Intermetallics*, vol. 4, no. 3, pp. 217–229, Jan. 1996.

[19] C. . Koch, “Intermetallic matrix composites prepared by mechanical alloying—a review,” *Mater. Sci. Eng. A*, vol. 244, no. 1, pp. 39–48, Mar. 1998.

[20] J. Doychak, “Metal- and intermetallic-matrix composites for aerospace propulsion and power systems,” *JOM*, vol. 44, no. 6, pp. 46–51, Jun. 1992.

[21] K. S. Kumar and G. Bao, “Intermetallic-matrix composites: An overview,” *Compos. Sci. Technol.*, vol. 52, no. 2, pp. 127–150, Jan. 1994.

[22] R. Kainuma, Y. Fujita, H. Mitsui, I. Ohnuma, and K. Ishida, “Phase equilibria among α (hcp), β (bcc) and γ (L10) phases in Ti–Al base ternary alloys,” *Intermetallics*, vol. 8, no. 8, pp. 855–867, Aug. 2000.

[23] Y. Tsunekawa, K. Gotoh, M. Okumiya, and N. Mohri, “Synthesis and high-temperature stability of titanium aluminide matrixin situ composites,” *J. Therm. Spray Technol.*, vol. 1, no. 3, pp. 223–229, Sep. 1992.

[24] K. P. Plucknett and P. F. Becher, “Processing and Microstructure Development of Titanium Carbide – Nickel Aluminide Composites Prepared by Melt Infiltration / Sintering (MIS),” vol. 61, pp. 55–61, 2001.

[25] K. P. Plucknett, P. F. Becher, and R. Subramanian, “Melt-infiltration processing of TiC/Ni3Al composites,” *J. Mater. Res.*, vol. 12, no. 10, pp. 2515–2517, Oct. 1997.

[26] T. L. Stewart and K. P. Plucknett, “The sliding wear of TiC and Ti(C,N) cermets prepared with a stoichiometric Ni3Al binder,” *Wear*, vol. 318, no. 1–2, pp. 153–167, Oct. 2014.

[27] P. Sahoo and M. J. Koczak, “Microstructure-property relationships of in situ reacted TiC/Al□Cu metal matrix composites,” *Mater. Sci. Eng. A*, vol. 131, no. 1, pp. 69–76, Jan. 1991.

[28] S.-H. Ko, B.-G. Park, H. Hashimoto, T. Abe, and Y.-H. Park, “Effect of MA on microstructure and synthesis path of in-situ TiC reinforced Fe–28at.% Al intermetallic composites,” *Mater. Sci. Eng. A*, vol. 329–331, pp. 78–83, Jun. 2002.

[29] M. Krasnowski, A. Witek, and T. Kulik, “The FeAl–30%TiC nanocomposite produced by mechanical alloying and hot-pressing consolidation,” *Intermetallics*, vol. 10, no. 4, pp. 371–376, Apr. 2002.

[30] R. Subramanian and J. . Schneibel, “FeAl–TiC and FeAl–WC composites—melt infiltration processing, microstructure and mechanical properties,” *Mater. Sci. Eng. A*, vol. 244, no. 1, pp. 103–112, Mar. 1998.

[31] R. Subramanian and J. . Schneibel, “FeAl-TiC cermets—melt infiltration processing and mechanical properties,” *Mater. Sci. Eng. A*, vol. 239–240, pp. 633–639, Dec. 1997.

[32] C. L. Cramer, A. D. Preston, A. M. Elliott, and R. A. Lowden, “Highly dense, inexpensive composites via melt infiltration of Ni into WC/Fe preforms,” *Int. J. Refract. Met. Hard*

Mater., vol. 82, pp. 255–258, Aug. 2019.

[33] C. A. Leon, V. H. Lopez, E. Bedolla, and R. A. L. Drew, "Wettability of TiC by commercial aluminum alloys," *J. Mater. Sci.*, vol. 37, no. 16, pp. 3509–3514, 2002.

[34] L. Agudo *et al.*, "Intermetallic FexAly-phases in a steel/Al-alloy fusion weld," *J. Mater. Sci.*, vol. 42, no. 12, pp. 4205–4214, Jun. 2007.

[35] F. Stein, S. C. Vogel, M. Eumann, and M. Palm, "Determination of the crystal structure of the ε phase in the Fe–Al system by high-temperature neutron diffraction," *Intermetallics*, vol. 18, no. 1, pp. 150–156, Jan. 2010.

[36] X. Li, A. Scherf, M. Heilmaier, and F. Stein, "The Al-Rich Part of the Fe-Al Phase Diagram," *J. Phase Equilibria Diffus.*, vol. 37, no. 2, pp. 162–173, Apr. 2016.

[37] G. F. Bastin, F. J. J. van Loo, J. W. G. A. Vrolijk, and L. R. Wolff, "Crystallography of aligned Fe-Al eutectoid," *J. Cryst. Growth*, vol. 43, no. 6, pp. 745–751, Jul. 1978.

[38] K. Frisk, "A revised thermodynamic description of the Ti–C system," *Calphad*, vol. 27, no. 4, pp. 367–373, Dec. 2003.

[39] W. Zhang, N. Bay, and T. Wanheim, "Influence of hydrostatic Pressure in Cold-Pressure Welding," *CIRP Ann.*, vol. 41, no. 1, pp. 293–297, Jan. 1992.

[40] C. W. Bale *et al.*, "FactSage thermochemical software and databases," *Calphad*, vol. 26, no. 2, pp. 189–228, Jun. 2002.

[41] Y. Du, J. C. Schuster, H. J. Seifert, and F. Aldinger, "Experimental Investigation and Thermodynamic Calculation of the TitaniumSiliconCarbon System," *J. Am. Ceram. Soc.*, vol. 83, no. 1, pp. 197–203, Jan. 2000.

[42] D. Bandyopadhyay, "The Ti-Si-C system (Titanium-Silicon-Carbon)," *J. Phase Equilibria Diffus.*, vol. 25, no. 5, pp. 415–420, Dec. 2004.

[43] T. Tsukahara, … N. T.-… O. T. I., and undefined 2016, "Mechanical Properties of Fe2Al5 and FeAl3 Intermetallic Phases at Ambient Temperature," *KAIKAN TEKKO KAIKAN-5F, 3-2-10 …*.

[44] "Intermetallics | Vol 54, Pages 1-242 (November 2014) | ScienceDirect.com."